Cell Mol Neurobiol (2012) 32:989–1001
DOI 10.1007/s10571-012-9815-5

ORIGINAL RESEARCH

Role of the Cellular Prion Protein in the Neuron Adaptation Strategy to Copper Deficiency

Emanuela Urso · Daniela Manno · Antonio Serra · Alessandro Buccolieri · Antonia Rizzello · Antonio Danieli · Raffaele Acierno · Benedetto Salvato · Michele Maffia

Received: 22 December 2011 / Accepted: 7 February 2012 / Published online: 24 February 2012

Abstract Copper transporter 1 (CTR1), cellular prion protein (PrP^C), natural resistance-associated macrophage protein 2 (NRAMP2) and ATP7A proteins control the cell absorption and efflux of copper (Cu) ions in nervous tissues upon physiological conditions. Little is known about their regulation under reduced Cu availability, a condition underlying the onset of diffused neurodegenerative disorders. In this study, rat neuron-like cells were exposed to Cu starvation for 48 h. The activation of Caspase-3 enzymes and the impairment of Cu,Zn superoxide dismutase (Cu,Zn SOD) activity depicted the initiation of a pro-apoptotic program, preliminary to the appearance of the morphological signs of apoptosis. The transcriptional response related to Cu transport proteins has been investigated. Notably, PrP^C transcript and protein levels were consistently elevated upon Cu deficiency. The CTR1 protein amount was stable, despite a two-fold increase in the transcript amount, meaning the activation of post-translational regulatory mechanisms. NRAMP2 and ATP7A expressions were unvaried. The up-regulated PrP^C has been demonstrated to enhance the cell Cu uptake ability by about 50% with respect to the basal transport, and so sustain the Cu delivery to the Cu,Zn SOD cuproenzymes. Conclusively, the study suggests a pivotal role for PrP^C in the cell adaptation to Cu limitation through a direct activity of ion uptake. In this view, the PrP^C accumulation observed in several cancer cell lines could be interpreted as a molecular marker of cell Cu deficiency and a potential target of therapeutic interventions against disorders caused by metal imbalances.

Keywords Copper deficiency · Adaptation · Neuroblastoma · Cellular prion protein · Copper transporters

E. Urso · A. Rizzello · A. Danieli · R. Acierno · M. Maffia (✉)
Department of Biological and Environmental Sciences and Technologies, University of Salento, SP Lecce-Monteroni, 73100 Lecce, Italy
e-mail: michele.maffia@unisalento.it

D. Manno · A. Serra · A. Buccolieri
Department of Material Sciences, University of Salento, SP Lecce-Monteroni, 73100 Lecce, Italy

B. Salvato
Department of Biology, University of Padova, Via U. Bassi 58/B, 35121 Padua, Italy

Background

Copper (Cu) has been established as an essential cofactor required by fundamental enzymatic and nonenzymatic pathways, including those involved in the defence of cells from oxidative damage (Cu,Zn superoxide dismutase, SOD), synthesis of ATP (cytochrome c oxidase), catecholamine (dopamine β-monooxygenase) and melanin production (tyrosinase), blood clotting processes (Factors V and VIII) and iron metabolism (ceruloplasmin and hephaestin) (Tapiero et al. 2003). The catalytic properties of Cu depend on its ability to easily assume the oxidized (Cu^{2+}) and the reduced (Cu^{+}) states, but just its redox chemistry can give rise to severe cellular alterations due to the production of highly reactive oxygen species (Halliwell and Gutteridge 1984, 1990). To limit the reactivity of this metal, living organisms developed a precise network of transporters and chaperons to properly address Cu ions toward specific compartments and molecules (Valentine and Gralla 1997; Pena et al. 1999; Bertinato and L'Abbé 2004; Kim et al. 2008). Cu-transporter 1 (CTR1) is a high affinity Cu^{+} importer spanning three trans-membrane

domains (Klomp et al. 2002). It exists as a homotrimer embedded in the lipid bilayer and a pore allows the ion translocation across the cell membrane (Nose et al. 2006; Lee et al. 2000; Zhou and Gitschier 1997; Aller and Unger 2006). Another candidate to drive Cu intake is the divalent metal transporter 1 (DMT1/NRAMP2) (Gunshin et al. 1997), demonstrated to sustain at least the 50% of Cu transport in Caco-2 cells, transporting both the Cu^{+} and the Cu^{2+} species (Arredondo et al. 2003). The cell surface protein cellular prion protein (PrP^{C}), mostly expressed by neurons at synapses and gliocytes (Salès et al. 1998; Brown et al. 1998), is also believed to influence Cu uptake, since the binding of Cu^{2+} ions to its extracellular N-terminal domain stimulates the protein endocytosis, possibly providing a way for cell Cu entry (Pauly and Harris 1998; Perera and Hooper 2001; Harris 1999; Brown 2001). Inside the cell, Cu is delivered to proteins and organelles by specific Cu chaperons targeting it to Cu,Zn SODs (CCS), cytochrome *c* oxidase (COX17) and the cytosolic domain of Cu-ATPases ATP7A and ATP7B, responsible for Cu-loading onto cuproproteins in the Golgi apparatus and export of ion excess (Markossian and Kurganov 2003; Lutsenko and Petris 2002; Linz and Lutsenko 2007).

Imbalances in ion homeostasis at both cellular and systemic levels are linked to symptoms associated to several neurodegenerative disorders, including Alzheimer's, Parkinson's, amyotrophic lateral sclerosis and prion diseases (Donnelly et al. 2007; Gaggelli et al. 2006; Gaeta and Hider 2005; Strausak et al. 2001). Some investigations revealed a role of plasma Cu deficiency in promoting the cognitive decline in Alzheimic subjects (Kessler et al. 2006; Pajonk et al. 2005). In addition, the oral administration of Cuprizone (Cu chelating agent) to mice has been shown to induce some histopathological features associated to prion infection (Kimberlin 1974; Pattison and Jebbett 1971a, b).

To examine in detail the molecular events occurring under Cu depletion independently on causal events, experimental models were set up, in the attempt to resemble a condition shared by several neurodegenerative disorders. In previous studies, Cu-related pathways were stressed in cultured neuroblastoma cells exposed to Cu chelating agents (Bathocuproine sulphonate, trientine) and research focused on the induction of oxidative stress and the activation of the apoptosis program (Lombardo et al. 2003; Rossi et al. 2001). No attention was devoted to the effects evoked on Cu transport systems.

In the attempt to go deep in this basic aspect, the main objective of this study was defining in a Cu-depleted neuronal-like cell line (B104) the relative contributions of well-known (CTR1, NRAMP2, ATP7A) and presumed (PrP^{C}) Cu-transporters to the cell adaptive response, in terms of transcriptional and post-translational regulation. The kinetics of Cu uptake during adaptation have been analysed by a fluorimetric method, in order to establish, if possible, a hierarchy in the intervention of the cited Cu-related proteins. In addition, the cell antioxidant status has been studied, with particular reference to the Cu,Zn SOD cuproenzyme activity.

Materials and Methods

Cell Culture and Treatments

B104 neuroblastoma cells, derived from rat central nervous system (Schubert et al. 1974), were grown at 37°C, 5% CO_2, in Dulbecco's-modified Eagle's medium (Euroclone Life Science, Milan, Italy), 1 g/l glucose, supplemented with 10% foetal bovine serum, 1 mM Na-pyruvate, 2 mM glutamine and antibiotics (penicillin/streptomycin 5,000 U/ml/5 mg/ml; Sigma-Aldrich, Milan, Italy).

To deprive cells of Cu, cultures were exposed to 15 μM triethylenetetramine dihydrochloride chelating agent (Trientine, Trien; Sigma-Aldrich, Milan, Italy) for 48 h. They were then processed for subsequent analysis.

To prevent clathrin-dependent endocytosis, cells were pre-incubated with 50 μM chlorpromazine hydrochloride (CPZ; Sigma-Aldrich) for 30 min or with hypertonic sucrose (0.5 M) for 20 min.

MTT Assays

A preliminary set of cell viability tests was performed, to define the more suitable conditions to study the events triggered by ion deficiency in the absence of covering effects due to Trien self-toxicity and a massive cell loss. To this aim, cells were plated into 96-well trays and exposed to growing concentrations (0–100 μM) of Trien for 48 and 96 h. As a control, cultures were simultaneously exposed to Cu–Trien complex (1:1 molar ratio).

0.5 mg/ml MTT [3-(4,5-dimethylthiazol-2-yl)-2,5-diphenyl-tetrazolium bromide; Sigma-Aldrich] was added to cell cultures for 3 h at 37°C. The MTT formazan product was released from cells by adding dimethylsulfoxide and measured spectrophotometrically at 570 nm (Mosmann 1983). The percent of survival was assessed by comparison with untreated cultures.

Determination of Total Copper (Cu), Zinc (Zn) and Iron (Fe) Cell Contents by Atomic Absorption Spectroscopy (AAS)

Cells grown in 60-mm dishes were repeatedly washed, lysed and digested in suprapur HNO_3 (0.2% v/v). Metal contents of solutions were measured by a Varian AA-600Z

atomic absorption spectrophotometer (Varian Inc., Australia), equipped with a GTA-100 graphite tube atomizer with Zeeman background correction and a PSD-120 autosampler. The detection wavelengths were set at 327.4 nm for Cu, 213.9 nm for Zn and 248.3 nm for Fe. Data were analysed by the Varian SpectrAA 3.10 FS software and metal concentrations were expressed as the weight of metal per milligram of proteins (nmol/mg protein). Three samples have been assayed for each quantification.

Caspase Activity Assay

Caspase-3 activity was measured using the ApoTarget™ Caspase-3 Protease Assay (BioSource International, Inc., Camarillo, CA, USA) according to the manufacturer's instructions. Briefly, cells were treated with 15 μM Trien for 48 h. Aliquots of cell lysates (150 μg protein per sample) were mixed with a reaction buffer containing 200 μM DEVD-*p*NA, a chromogen substrate and incubated for 2 h at 37°C in the dark. Absorbance values were measured at 405 nm and reported as a percentage of readings from the uninduced samples.

SOD Activity

B104 cells were treated as indicated in "Results" section. SOD activity was measured by the SOD Assay Kit-WST (Fluka, Sigma-Aldrich). This colorimetric assay relies on two concatenated reactions: the generation of superoxide anions (O_2^-) through the xanthine/xanthine oxidase system and the conversion of WST-1 [2-(4-iodophenyl)-3-(4-nitrophenyl)-5-(2,4-disulfophenyl)-2H-tetrazolium, monosodium salt] tetrazolium salt to a yellow water-soluble formazan dye following reduction by O_2^-. SOD activity inhibits the generation of the coloured salt by subtracting superoxide anions to reduction. Briefly, 20 μl lysates (sample wells) were dispensed in triplets into 96-well microplates. Then, 200 μl WST working solution and 20 μl enzyme working solution (xanthine/xanthine oxidase system) were added to wells.

Six blank wells (three for blank 1 and three for blank 2) per microplate were reserved. For blank 1, 20 μl water were added in place of samples. For blank 2, the enzyme working solution was substituted by 20 μl dilution buffer.

After 20 min incubation at 37°C, the absorbances at 450 nm were registered. SOD activity was calculated as the percent inhibition of WST-1 reduction with O_2^-, using the formula:

$$\text{SOD activity} = \left\{ \left[(A_{\text{blank1}} - A_{\text{blank2}}) - A_{\text{sample}} \right] / (A_{\text{blank1}} - A_{\text{blank2}}) \right\} * 100$$

Results were normalized against cell number.

Atomic Force Microscopy (AFM)

Images were acquired from 4% paraformaldehyde-fixed control and Cu-depleted cultures by an A Jeol 4210 STM-AFM microscope. Contact-mode cell images were taken in air at room temperature. Silicon cantilevers with 100-μm length, curvature radius <25 nm and spring constant of 0.05 N/m were used.

Real-Time PCR

RNA extraction from cells grown at 70–80% confluence was performed by using the TRIzol reagent (Invitrogen, Milan, Italy), accordingly to the manufacturer's instructions. Total RNA (0.5 μg) was reverse-transcribed with random hexamers in a 20 μl reaction volume by the GeneAmp® Gold RNA PCR kit (Perkin-Elmer, Monza, Italy). Amounts of cDNA template from 0.2 to 0.5 μg were needed for real-time PCR analysis. The primers used for selected transcripts, listed in Table 1, have been designed using the free National Center for Biotechnology

Table 1 Real-time PCR primer sequences and conditions

Target gene (protein) GenBank accession no.	Primers (sense, antisense)	T_m (°C)	PCR product size (bp)
Rat *Slc31a1* (CTR1)	5′-GGAGAAATGGCTGGAGCTTTT-3′	54	71
NM_133600	5′-CGGGCTATCTTGAGTCCTTCA-3′		
Rat *Slc11a2* (NRAMP2)	5′-CACTGTGATGCAAAGTCCT-3′	58	95
NM_013173	5′-CGCAGCCTGGTCTCAAG-3′		
Rat *Prnp* (PrP^C)	5′-ACTGGCTGCTGGCCCTCTTT-3′	58	101
NM_012631	5′-AGGGTACCGGCTTCCACCAG-3′		
Rat *Atp7A* (ATP7A)	5′-AAGCCAACATATGACAATTATGAGTTG-3′	54	78
NM_052803	5′-GTGAACGCTGATTTCTGAAGGA-3′		
Rat *Gadph* (GADPH)	5′-CTGCTCCTCCCTGTTCTAGAGACA-3′	58	105
NM_017008	5′-CCGATACGGCCAAATCCGTTCACA-3′		

Information (NCBI) tool Primer-BLAST, available at http://www.ncbi.nlm.nih.gov/tools/primer-blast.

Reactions were carried out into a 25-µl mixture volume using the SmartCycler® System (Cepheid, Euroclone, Milan, Italy) and the threshold cycles (C_t) were averaged from three samples, each analysed in duplicate. The average expression ratio of genes with respect to the control condition was computed by Pfaffl's formula (2001).

Western Blotting

Total proteins were isolated from cell cultures by the TRIzol protocol (Invitrogen). Aliquots to be analysed for prion protein expression were deglycosylated by PNGase F treatment for 3 h at 37°C (Enzymatic Protein Deglycosylation kit, Sigma-Aldrich). 30–100 µg proteins were loaded and run onto 7–12% SDS polyacrylamide gels. Separated protein bands were transferred onto nitrocellulose membranes at 190 mA for 1.5 h. After blocking with PBS-0.1% Tween containing 5% nonfat milk, membranes were incubated with primary antibodies raised against CTR1 (1:2000, Novus Biologicals), NRAMP2 (1:1000; Santa Cruz Biotechnology, Inc.), PrP^C (1:8000; Sigma-Aldrich), ATP7A (1:1000; Orbigen) overnight at 4°C and then with antirabbit (CTR1, NRAMP2, ATP7A) and antimouse (PrP^C) peroxidase-labelled secondary antibodies (Santa Cruz Biotechnology, Inc.) at room temperature for 1 h. After washes in PBS-0.1% Tween, band detection was performed by a horseradish peroxidase-based chemiluminescent detection system (ECL, Amersham). Results were normalized against β-actin.

Transport Measurements

The kinetics of Cu intake were studied in B104 cells after 48 h Trien treatment by a fluorimetric method, using the green-fluorescent heavy metal indicator Phen Green SK diacetate (PG SK, $\lambda_{exc} = 506$ nm, $\lambda_{em} = 530$ nm; Molecular Probes, Invitrogen). Cells were harvested and then dye-loaded by incubation for 10 min at 37°C in HBSS (in mM: 140 NaCl, 5 KCl, 1 Na_2HPO_4, 1 $CaCl_2$, 0.5 $MgCl_2$, 5 D-glucose, 10 Hepes; pH 7.4) containing 1 µM PG SK. After loading, cells were washed twice by centrifugation and then resuspended in the physiological buffer cited above. For each evaluation, an aliquot of cells (3×10^4) was introduced in a cuvette housed in a LS-50B Perkin-Elmer spectrofluorometer, after the preheating of the sample compartment at 37°C. Once the emission signal of the probe "entrapped" within the cells was stable, Cu chloride was added at different concentrations (0–5 µM) and the rate of fluorescence quenching (ΔF a.u. s^{-1} nr $cells^{-1}$ 10^{-5}) was monitored as an indicator of Cu influx rate into the cytoplasm.

A set of experiments was conducted on both untreated and Cu-depleted cells, before and after the enzymatic removal of surface PrP^C. In the last case, cultures were washed twice with phosphate-buffered salt solution and then pre-incubated in serum-free medium containing 5 mU/cm^2 phosphatidylinositol-specific phospholipase C (PI-PLC) from *B. cereus* (Sigma-Aldrich) for 2.5 h at 37°C. Cells were dye-loaded as reported above and Cu transport assays performed by testing single extracellular Cu concentrations in separate experiments. The absolute Cu intake was computed as $\Delta F_{max}/F_0$ ratio, where ΔF_{max} is the maximum change in fluorescence observed after the addition of Cu to cells and F_0 is the baseline signal, and expressed as a percentage of control.

Data Analysis

Results are presented as means ± SE and each experiment has been done at least in triplicate. Statistical comparisons have been made by Student's t test and ANOVA followed by Dunnett's post-test. Significance was demonstrated at $p < 0.05$ (*).

Results

Trientine Effects on Cell Viability and Cu Status

B104 cells were treated for 48 and 96 h with 0–100 µM Trien alone and in combination with equimolar $CuCl_2$, to consider a possible loss of cell viability due to the chelating agent self-toxicity. At the shortest treatment time, Trien did not show any toxicity per se even at the highest concentration (dark bars in Fig. 1a). A slight toxicity, even if not significant, was observed after 96 h treatment with 25 µM Cu:Trien, not further exacerbated at 100 µM (Fig. 1b), to indicate that a prolonged exposure to this agent can slightly affect B104 cell viability independently on Cu chelation. When Trien was administered alone, a significant toxicity was detected only after 96 h treatment at concentrations equal or over 15 µM (Fig. 1b). To study the effects precociously induced by Cu deficiency in B104 cultures, in the absence of events linked to a significant toxicity, we chose to test a condition preliminary to the loss of viability caused by 96 h treatment with 15 µM Trien. Studies were performed on cells cultured in the presence of 15 µM Trien for 48 h.

We observe that Trien binds Cu^{2+} ions selectively, but it also exhibits a lower affinity for Zn^{2+} and $Fe^{2+/3+}$ ions. To assess if the selected experimental conditions could significantly deplete the intracellular pools of other ions than Cu, total amounts of Zn, Fe and Cu were quantified by AAS in lysates prepared from control and 48 h Trien-treated cultures. Total Cu levels appeared reduced by more

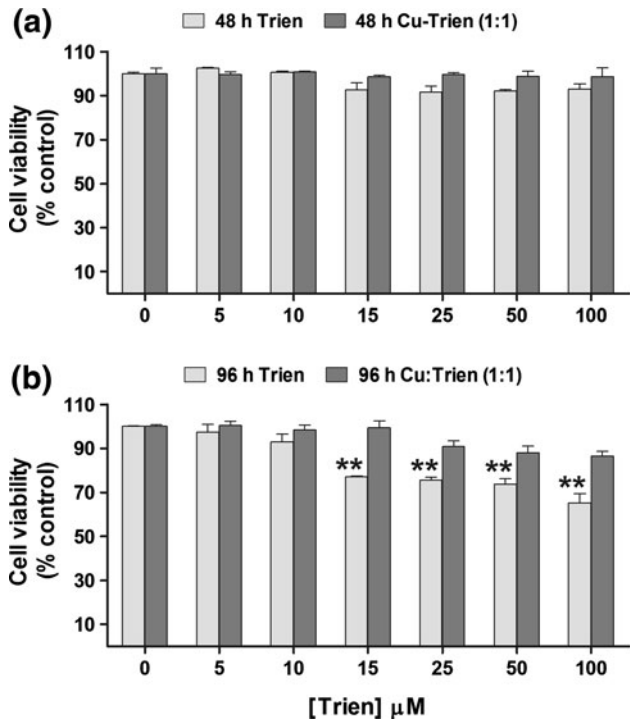

Fig. 1 Effects of Trien Cu chelating agent on B104 cell viability. MTT assays were performed on cultures treated with growing concentrations of Trien and Cu:Trien complex for 48 (**a**) and 96 (**b**) h. Experiments were repeated three times, with triplicate wells for each condition (mean ± SE; $^{**}p < 0.01$)

Table 2 Total Cu, Zn and Fe determination in cell lysates by AAS

	Cu (nmol/ mg protein) Mean ± SE	Fe (nmol/ mg protein) Mean ± SE	Zn (nmol/ mg protein) Mean ± SE
Untreated	0.24 ± 0.04	1.13 ± 0.01	2.10 ± 0.01
48 h Trien	0.10 ± 0.06	0.87 ± 0.16	2.12 ± 0.01

than a half with respect to control condition (Table 2). Fe levels resulted slightly, but nonsignificantly reduced, while Zn content was substantially unchanged (Table 2). These findings were expected, since preliminary AAS evaluations on standard growth media (containing foetal bovine serum from different batches) indicated that Cu abundance is at least one order of magnitude lower than observed for Zn and Fe (10^{-1} vs. 10). We adopted a Trien concentration well below the values reported in most literature (Spisni et al. 2009; Lombardo et al. 2003; Rossi et al. 2001), and reasonably able to "buffer" the small amount of dissolved Cu ions, while being not enough to significantly chelate Fe and Zn.

On the whole, cell viability assays and AAS data supported the choice of Trien as a tool to reproduce Cu deficiency in vitro, in the absence of confounding effects due to the limited availability of other metal ions.

Caspase-3 Activation

The caspase-3 protease activity was measured as an indicator of the induction of mechanisms possibly leading to apoptosis in Cu-deprived B104 cells. Following exposure of cultures to 15 μM Trien for 48 h, a rise in the protease activity was detected (about 1.5-fold; $p < 0.05$) (Fig. 2). The observation of treated cells by optical microscopy indicated that the initiation of cell death pathways was precocious with respect to the appearance of morphological changes typical of the apoptotic commitment, such as cell retraction and plasma membrane 'blebbing'. A more in-depth investigation of cell morphology under Cu starvation was conducted by AFM.

AFM Imaging

Surface topographies were obtained from fixed cultures, showing the height variations and highlighting the fine features of surface morphology. Figure 3 clearly shows that Trien treatment modifies the cell shape, inducing control cells (a and b) to lengthen (c and d).

To determine the Trien-treated cell size, we calculated the Feret diameter, defined as the average caliper distance of 36 measurements around the particle centre employing a 5° angle of rotation, and the R roundness factor, defined by the following formula:

$$R = P^2/4\pi A,$$

where the object area A is defined by the number of pixels having intensity values within a selected range and the

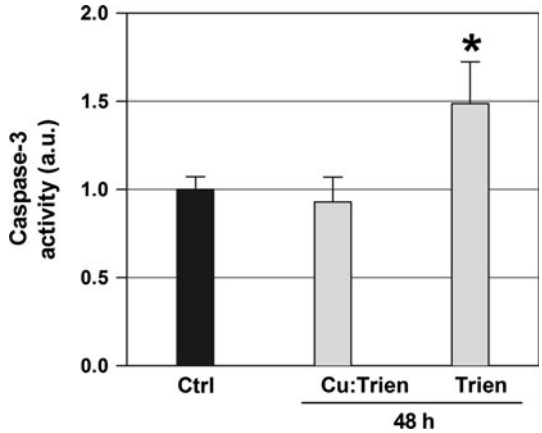

Fig. 2 Caspase-3 activity in B104 cells exposed to Cu deprivation. Neuroblastoma cells were treated with 15 μM Trien for 48 h. Caspase-3 activation was evaluated on fresh cell homogenates by a colorimetric method based on the enzymatic cleavage of the chromogen substrate DEVD-*p*NA (λ_{em} 405 nm). The activity was graphed in terms of arbitrary units, assuming the control value as datum-point (1 a.u.). Results are the mean ± SE of three separate assays ($^{*}p < 0.05$)

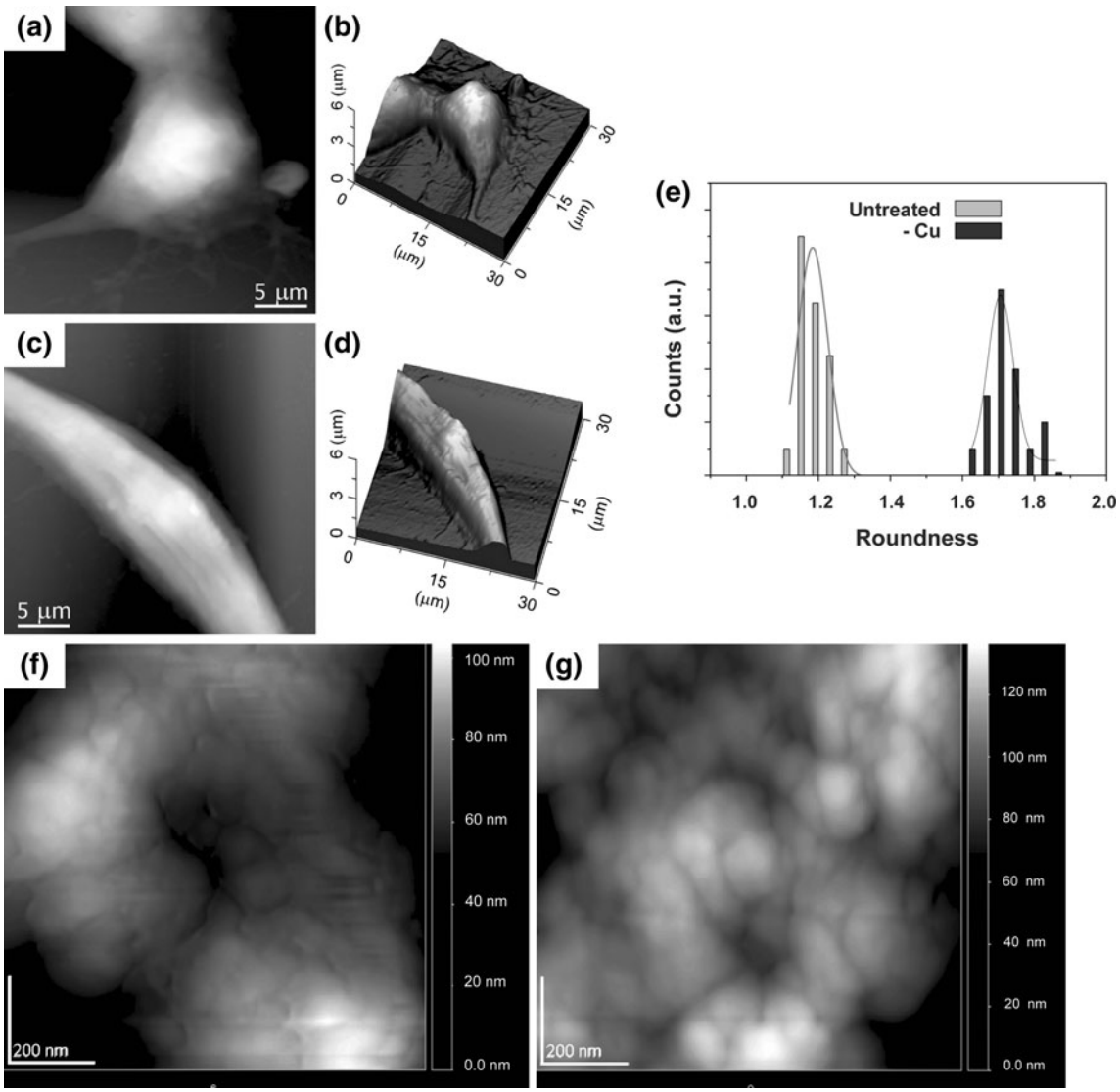

Fig. 3 Effects of Trien on cell morphological features. AFM pictures (**a**–**d**) of **a**, **b** untreated and 48 h **c**, **d** Trien-treated cells over a scan area of 30 × 30 μM^2. Measurements have been carried out in contact mode. **e** Roundness histograms for each experimental condition are shown. The peaks of the Gaussian curves identify the mean roundness factor for control and treated cells. **f**, **g** High-resolution AFM images of cell membrane roughness before (**f**) and after (**g**) the 48 h pre-incubation with Trien. The brightness of cell surface areas is an index of the cell height

perimeter P is defined by the outline length of each particle. Smooth and round objects have a roundness factor close to 1 unity, while elliptical objects have roundness factors >1 as they are elongated (Nazar et al. 1996). The histograms in Fig. 3e show the roundness of untreated cells (light shaded) with respect to Cu-depleted ones (dark shaded). In both cases the histograms are fitted by a Gaussian profile (superimposed as a solid line). The roundness values that best interpolate the experimental data are 1.18 ± 0.05 and 1.71 ± 0.06 units for control and treated cultures, respectively.

The nanomolar resolution AFM images in Fig. 3f, g evidently show that the surface of treated cells (g) exhibits a pronounced roughness with respect to untreated ones (f), demonstrating the alteration of cell molecular structures following Cu deprivation. For each condition, the AFM images were recorded from both the nuclear and the cytoplasmic regions of at least five cells.

Gene and Protein Expression of Cu-Transporters

Quantitative real-time PCR analysis was carried out to analyse the transcript content of the main Cu-transporters in Trien-treated B104 cells. Following normalization to GADPH, the relative mean expression rate of transcripts was compared between control and 48 h Cu-depleted cells.

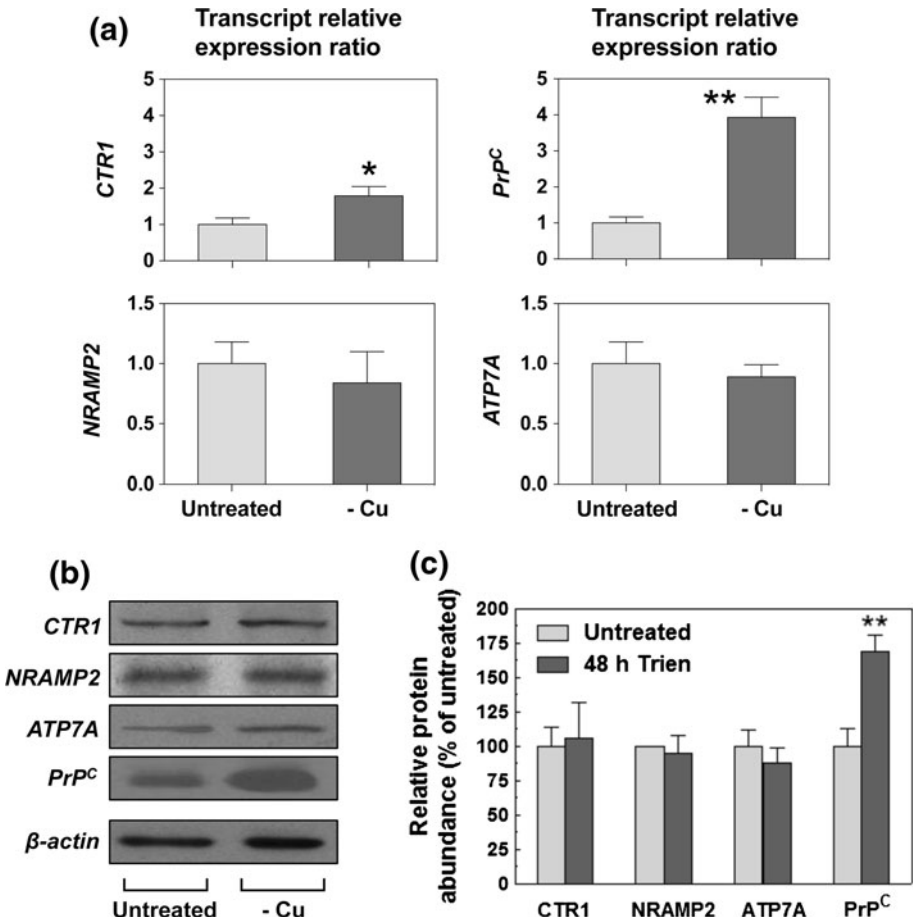

Fig. 4 Analysis of the expression of Cu-transporters in Trien-treated B104 cells. **a** The real-time PCR analysis of total RNA isolated from control and Cu-deprived B104 cells demonstrated that PrP^C and CTR1 mRNA levels are significantly increased following exposure to Trien for 48 h ($*p < 0.05$; $**p < 0.01$, ANOVA), whereas NRAMP2 and ATP7A mRNA levels are unaffected ($*p > 0.05$). A quantitative measurement of the messenger expression ratio relative to untreated cells has been done for each gene using the Pfaffl's formula. Data have been normalized to the expression of the housekeeping gene *Gadph* and they are expressed as mean ± SE from three separate experiments, each made in duplicate. **b** Protein extracts from treated cultures were subjected to western blot analysis to detect CTR1, PrP^C, NRAMP2 and ATP7A proteins. Blots are representative of three separate assays. The mean protein abundances resulted unaffected for CTR1, NRAMP2 and ATP7A ($p > 0.05$). A specific band of 30 kDa can be observed for prion protein, consistently more intense for treated samples ($**p < 0.01$). **c** Variation in the amounts of proteins with Trien exposure ($n = 3$). Band intensities were quantified using *Image J software*

The mean expression of NRAMP2 and ATP7A transporters was not significantly different ($p > 0.05$) in Cu-deprived cells with respect to control cultures (Fig. 4a), while a significant increase of CTR1 mRNA levels was observed ($p < 0.05$). Such result was highly reproducible, as confirmed by the low inter-assay variability, described by a coefficient of variation (CV%) ranging from 0.63 for 48 h treatment to 1.30 for control condition. In addition, a heavy effect on PrP^C transcript content was observed. Data shown in Fig. 4a highlight that Cu deprivation resulted in a four-fold increase in transcript levels for the PrP^C after Trien treatment (CV% 0.96).

The protein amounts of Cu-transporters were determined by immunoblot analysis. As pertains to CTR1 protein, the antibody utilized in this study specifically detected a band with the apparent size of the trimeric form (127 kDa) (Fig. 4b), as revealed in other cell models and mammalian tissues (Kelleher and Lönnerdal 2006; Hardman et al. 2006). The densitometric quantification indicated that the expression of CTR1 protein was unchanged in treated cells (Fig. 4c), although an activation of transcription was appreciable, evidencing the possibility that Cu can act as a post-translational modulator in mammalian cells. Western blot results did not show any substantial change in NRAMP2 and ATP7A protein synthesis by Cu-depleted cells ($p > 0.05$; Fig. 4b, c). On the contrary, consistently with real-time PCR results, prion protein expression appeared to be up-regulated. An about 70% increase in PrP^C expression with respect to control condition was observed after treatment ($p < 0.01$; Fig. 4b, c).

Cu Transport in Ion-Depleted Cultured Cells

A kinetic study of Cu transport was performed on control and 48 h Trien-treated cultures by a fluorimetric method based on the Cu-sensitive probe Phen Green SK (Urso et al. 2010).

The kinetic curve obtained for treated cells appeared similar to the control one and assimilable to a hyperbole (Fig. 5a), but the Michaelis–Menten constant (K_m) was heavily reduced and the maximal velocity (V_{max}) significantly increased (see Table 3). The ion transport efficiency, calculated as V_{max}/K_m ratio, was almost four-fold higher in Cu-depleted cells if compared to untreated ones (see Table 3).

To verify if other proteins than PrP^C might account for the higher Cu uptake ability, the ion transport activity was measured in both control and Cu-depleted cells, after the enzymatic removal of surface PrP^C molecules by PI-PLC. The histogram in Fig. 5b, referred to 0.8 μM extracellular Cu, is representative of all concentrations considered for the kinetic analysis, with slight quantitative variations. Under standard conditions, PrP^C has been shown to be responsible for the 32.41 ± 2.56% of the absolute Cu intake (see 'Ctrl' and 'PLC' bars, Fig. 5b). This value reflects the reduction of ion transport activity after the enzymatic removal of surface PrP^Cs (*2* in Fig. 5b). After Trien treatment, the cell ability to import Cu ions has been demonstrated to be about double than normal (98.0 ± 0.2% increase), and then it was questioned if such variation was fully due to the observed consistent up-regulation of prion protein. When surface PrP^C proteins were removed from Trien-treated cells by PI-PLC, the Cu transport activity was only 18.4 ± 8.9% higher than observed in control cultures (*3* in Fig. 5b), this reflecting the loss of ion transport activity through both basal and up-regulated PrP^C. If the contribution of PrP^C under basal conditions is subtracted from the whole PrP^C-dependent component of transport (*4* in Fig. 5b), it can be concluded that the increase of prion protein expression in Cu-deprived cells accounts for a 47.2 ± 9.3% surplus of Cu uptake.

Mechanisms associated to the (*3*) component of Cu transport activity in Trien and PI-PLC treated cells ('−Cu, PLC' bar, Fig. 5b) are PrP^C-independent and cannot be deduced from this study.

Dependence of SOD Activity on Prion Protein Expression

We investigated whether the up-regulated PrP^C in Cu-deprived cultures could influence the endogenous antioxidant buffer capacity, intended as SOD activity.

When B104 cells were Cu-starved for 48 h, a half-reduced level of SOD activity was observed with respect to control cultures (Fig. 6a). To explore the ability of Trien-treated cells to balance their antioxidant defences, cultures were switched to Trien-free standard medium for up to 4 h

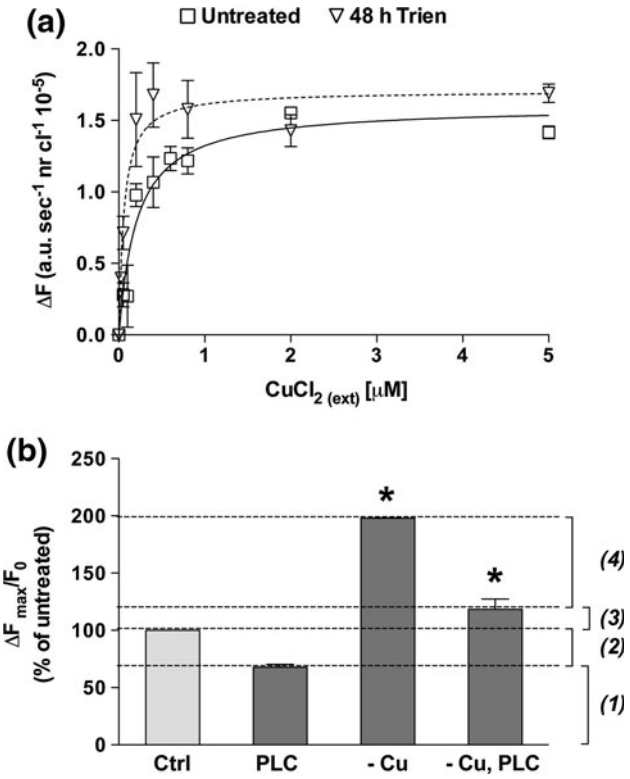

Fig. 5 Effect of Cu deprivation on ion transport kinetics. **a** Cu transport kinetics were studied after the pre-incubation of cultured cells in the presence of 15 μM Trien for 48 h. Cells were exposed to growing concentrations of $CuCl_2$ salt and the kinetic parameters of Cu uptake were determined using *GraphPad Prism version 5.00* (San Diego, California, USA). For each experimental condition, mean values of at least three experimental evaluations are shown. **b** Quantification of the absolute Cu intake in the presence of extracellular 0.8 μM $CuCl_2$ in control (Ctrl) and Trien-treated (−Cu) cells, before and after the enzymatic detachment of surface PrP^C molecules (PLC). Numbers flanking the histogram identify the various components of Cu transport under the two experimental conditions: PrP^C-independent (*1*) and PrP^C-dependent (*2*) contributions under basal conditions; PrP^C-independent (*3*) and PrP^C-dependent (*4*) components of the increase in Cu uptake following ion starvation. Experiments were repeated three times, with triplicates for each condition (mean ± SE; $*p < 0.05$)

(Fig. 6a, white bars). At the highest time point, the decreased enzyme activity resulted nearly fully restored (90.5 ± 4.0% of control). When PrP^C molecules were enzymatically cleaved from the surface of Cu-starved cells, the ability to recover SOD activity was compromised (Fig. 6a, grey bars).

It was investigated if the PrP^C-dependent recovery of cell SOD activity upon Cu replenishment was due to a protein inherent SOD-like function or to the enhanced Cu influx and loading of antioxidant enzymes. To this aim, Cu-deprived cells were exposed to CPZ and hypertonic sucrose, to prevent the PrP^C-mediated uptake of Cu ions occurring through the clathrin-dependent endocytic pathway (Urso et al. 2010). After treatments, cultures were maintained in standard growth medium for 4 h and SOD

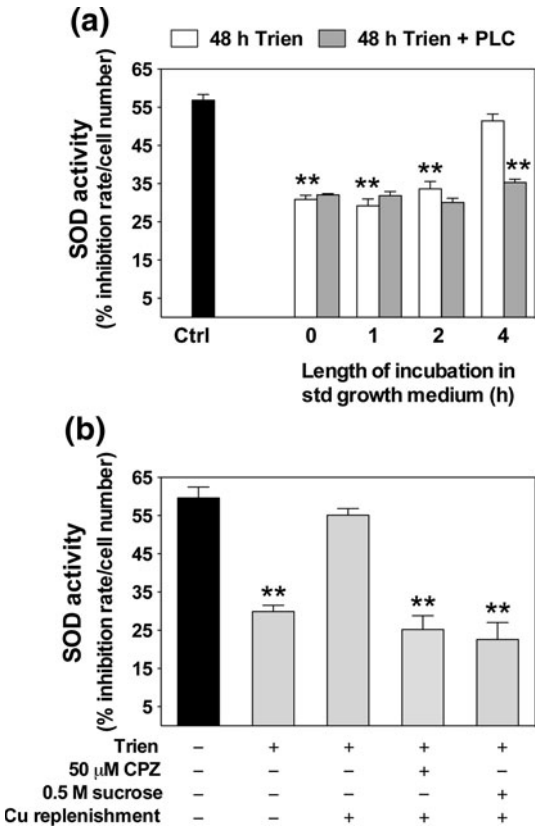

Fig. 6 PrP^C expression modulates the Cu,Zn SOD activity. **a** PrP^C-dependent recovery of the impaired SOD activity under Cu deficiency. 15 μM Trien-treated B104 cells were grown in standard growth medium for 1–4 h before and after the exposure to PI-PLC for 2.5 h at 37°C. SOD activity was then calculated as the rate of inhibition of xanthine/xanthine oxidase reduction of WST-1 and compared with the value obtained for untreated cultures. **b** Dependence of SOD activity on endocytic PrP^C-driven cell Cu uptake. SOD activity was determined in 15 μM Trien-treated cells (Trien), before and after the exposure of cultures to 50 μM CPZ for 30 min (CPZ) and 0.5 M sucrose for 20 min (0.5 M sucrose). Values have been expressed as mean ± SE of three measurements for each condition. $^{**}p < 0.01$ indicates a highly significant difference from control

activity was calculated. In both cases, the enzyme activity was the same as detected in Trien-treated cells without switching to the standard medium (Fig. 6b).

On the whole, these data indicate that the up-regulation of PrP^C induced by Cu deficiency in B104 cells is aimed to increase the intake of Cu ions and indirectly sustains the Cu,Zn SOD activity.

Discussion and Conclusions

The implication of Cu in the pathogenesis of a wide range of neurodegenerative diseases has become evident (Rivera-Mancía et al. 2010; Waggoner et al. 1999; Zatta and Frank 2007). Cu deficiency is likely to trigger neurological disturbances and physical lesions characterizing neurodegeneration (Zatta and Frank 2007), but the full comprehension of the molecular events underlying their onset has not been reached yet. In addition, a few studies have been dedicated to the role of Cu in modulating the transcriptional activities in cell cultures, under both ion deficiency and overload (Song et al. 2008, 2009; Muller et al. 2007; Ogra et al. 2006; Song and Freedman 2005; Tennant et al. 2002). Previous research on Cu-starved neuroblastoma cells privileged the link between the ion imbalance and the impairment of antioxidant cell activities, a risk factor for the onset of neurodegenerative disorders (Lombardo et al. 2003; Rossi et al. 2001).

In this work, an in vitro analysis of neuron cell response to Cu deficiency was reported, with significant attention paid to the expression of Cu plasma membrane transporters and the oxidative status (antioxidant activity). A neuroblastoma cell model, B104, was used, mimicking the physiological characteristics of neurons and expressing high levels of prion protein with a glycosylation pattern comparable to that of an adult brain (Monnet et al. 2003; Schubert et al. 1974). The cytosolic Cu pools have been depleted by treating cultures with the Cu chelating agent trientine, demonstrated to efficaciously stress the Cu-dependent cellular pathways (Spisni et al. 2009; Lombardo et al. 2003; Moriguchi et al. 2002; Zerounian and Linder 2002; Rossi et al. 2001; Yu and Wessling-Resnick 1998).

Preliminary investigations showed a significant increase of caspase-3 activity in Cu-starved cells, indicating the activation of a cell death program through the induction of oxidative stress. In fact, among cysteine proteases, caspase-3 enzymes have the heaviest impact when the ROS generation exceeds the antioxidant cell defences (Jiménez Del

Table 3 Kinetic parameters determined from Cu uptake curves in B104 cell model under control conditions and after 48 h Trien treatment

	K_m (μM) Mean ± SE	V_{max} (a.u. s^{-1} nr $cells^{-1}$ 10^{-5}) Mean ± SE	Catalytic efficiency (a.u. s^{-1} nr $cells^{-1}$ 10^{-5}/μM) Mean ± SE
Untreated	0.21 ± 0.03	1.6 ± 0.06	7.62 ± 0.15
48 h Trien	0.06 ± 0.01**	1.70 ± 0.05*	28.33 ± 0.17*

The Michaelis–Menten constant and the maximal velocity were calculated by nonlinear regression analysis with Graphpad Prism software version 5.0. Criteria for significance: * $p < 0.05$, ** $p < 0.01$

Río and Vélez-Pardo 2004; Rossi et al. 2001; Matsura et al. 1999). Surprisingly, the nano-scale AFM images (Fig. 3) did not show any typical morphological signs of advanced apoptosis, as cell shrinkage and cytoplasmic 'blebbing'. Cu-depleted cells generally appeared spindle-shaped and showed a marked plasma membrane roughness, not associated with changes in cell height (Fig. 3). This last morphological feature generally correlates with changes in the expression of surface proteins (Francis et al. 2009). Accordingly, the analysis of mRNA and protein abundance in treated B104 cells showed the heavy induction of a surface protein, PrP^C, whose role as a cell adhesion molecule could also explain the neurite outgrowth and cell elongation that we observed (Santuccione et al. 2005).

A major section of this study centres on the transcriptional response activated by Cu starvation. As previously disclosed, a striking elevation of PrP^C transcript and protein levels has been evidenced in 48 h Cu-depleted B104 cells (Fig. 4), this indicating a significant involvement of prion protein in maintaining cell Cu homeostasis.

Conflicting views coexist in the literature about the modulation of PrP^C expression in response to an altered Cu availability. Varela-Nallar et al. (2006) documented the ability of Cu to reversibly induce the *P-rnp* gene expression in primary hippocampal and cortical neurons. Cultured fibroblasts with a genetic defect in Cu efflux have also been found to up-regulate the *P-rnp* gene expression under chronic Cu overload (Armendariz et al. 2004). On the contrary, the down-regulation of PrP^C expression has been observed in Cu-treated hypothalamic neurons (Toni et al. 2005), meaning that the regulatory mechanisms depend on cell type. It is unlikely that cell-specific transcription factors are responsible for such variability, since those notoriously involved in *P-rnp* gene expression (Sp1, MTF-1, Ap-1, Ap-2, Atox-1) are ubiquitous (Bellingham et al. 2009; Mahal et al. 2001; Wright et al. 2009). Based on previous epigenetic studies (Cabral et al. 2002), a possible explanation could be that Cu deficiency acts in concert with unidentified cell-specific and ion-sensitive factors to disrupt the chromatin assembly and allow the accession of transcription factors to the *P-rnp* gene promoter.

To explain the considerable increase of PrP^C expression detected in Cu-deficient B104 cells, a compensatory role has been proposed for the up-regulated protein, aimed to restore the cell Cu status through the enhancement of PrP^C-mediated ion intake processes.

The ability of PrP^C to promote Cu delivery is currently highly debated. PrP^C has been reported to undergo endocytosis upon Cu binding (Perera and Hooper 2001; Pauly and Harris 1998; Brown et al. 1997a) and increase the cell Cu content in brain fractions (Brown 2003; Herms et al. 1999). However, in vitro studies demonstrated that PrP^C functions as a Cu importer only under high ion concentration (Rachidi et al. 2003).

Previous studies from our laboratory in B104 cell model upon physiological conditions gave a proof of a PrP^C-dependent component of Cu intake through clathrin-dependent endocytosis (Urso et al. 2010). To investigate the function of PrP^C upon Cu deprivation, the characteristics of Cu transport have been analysed in ion-depleted B104 cells. The 48 h trientine treatment, besides increasing the PrP^C expression, resulted in an enhancement of cell transport activity, as confirmed by a nearly four-fold increase of the catalytic efficiency. The K_m value determined for Cu-deprived cells was significantly reduced (about 3.5-fold) and the maximal velocity increased by about 6% with respect to the control value, this indicating the presence of a greater number of Cu-transporters on the cell surface. Based on this experimental evidence and our previous work showing a role for PrP^C in mediating Cu transport (Urso et al. 2010), the detected increase in the uptake activity has been supposed to be mainly dependent on a consistent contribution from surface prion proteins. Accordingly, when these proteins have been enzymatically released from Cu-depleted cells, the cell ability to bring Cu ions in was close to basal levels. An about 50% of surplus Cu intake has been estimated to be mediated by the up-regulated PrP^C (Fig. 5).

We have also considered the hypothesis that the newly synthesized prion protein up-regulates the activity of other proteins, like SODs, to balance the generation of ROS induced by Cu chelation (Lombardo et al. 2003; Rossi et al. 2001). Accordingly, the ^{64}Cu loading and the enzymatic activity of Cu,Zn SOD from the brain of *P-rnp*$^{0/0}$ mice result 10-50% reduced with respect to the wild-type genotype (Klamt et al. 2001; Brown and Besinger 1998; Brown et al. 1997b).

The relationship between the expression of prion protein and the activity of the cuproenzyme Cu,Zn SOD has been re-examined in B104 cells upon Cu deprivation. The total SOD activity resulted half-reduced, as expected in consideration of the role of Cu as a Cu,Zn SOD cofactor. Based on literature evidences (Brown et al. 1997b, 1999, 2002), the overexpression of surface PrP^C has been interpreted as a cell adaptation strategy, functional to revert the impairment of Cu,Zn SOD activities. Accordingly, the up-regulated PrP^C has been demonstrated to be responsible for the ability of Cu-starved cells to almost completely recover the SOD enzyme function upon re-exposure to standard growth conditions. The cleavage of surface prion proteins in treated cells made them unable to restore the SOD activity despite the availability of Cu ions (Fig. 6).

It was questioned whether the uptake of Cu is a prerequisite for the PrP^C protective action against oxidative cell injury or this protein possesses a SOD-like activity.

When the endocytosis phenomena were inhibited in Trien-treated cells, the up-regulated PrP^C, even if in the presence of extracellular Cu, was not able to restore the basal SOD activity. This finding demonstrates that Cu-loaded PrP^C has not an inherent antioxidant activity, but its neuroprotective action is due to the ion translocation into the cytosol. Here, Cu ions can act as cofactors in Cu,Zn SOD activation.

The expression of CTR1 proteins has been also studied upon Cu starvation in B104 cultures. The protein abundance resulted unaffected, although the transcript was about doubled with respect to untreated cells, indicating the occurrence of post-translational control mechanisms.

To our knowledge, in just a few cases it has been demonstrated in vitro that the levels of CTR1 transcript are inversely correlated to Cu availability (Song et al. 2008; Ricciardo et al. 2009). Most literature reports evidence that CTR1 is not subjected to transcriptional regulation in vitro (Hardman et al. 2006; Bauerly et al. 2004; Tennant et al. 2002). The CTR1-mediated Cu entry in mammalian cells is prevailingly controlled in a post-translational way, through the Cu-stimulated degradation of transporters (Nose et al. 2010; Petris et al. 2003; Tennant et al. 2002). The discrepancy between mRNA and protein levels emerging from this study could be explained by an increased sensitivity of CTR1 to proteasome degradation, as observed for CTR2 in the presence of the apo-ATOX1 form (Blair et al. 2010).

As to NRAMP2, the unvaried levels of this transporter in Cu-starved cultures were unexpected, since this protein, recognized as a physiologically relevant Cu^+-transporter (Arredondo et al. 2003), is known to be subjected to transcriptional regulatory mechanisms, variously operated by Fe, Zn and Cu ions (Arredondo et al. 2004; Tennant et al. 2002; Zerounian and Linder 2002; Martini et al. 2002; Yamaji et al. 2001; Yeh et al. 2000). The ATP7A protein content was also unchanged in response to Cu depletion, in agreement with most literature. In fact, the activity of this pump is notoriously regulated through events of intracellular protein relocalization. It is well-known that the elevation of intracellular Cu triggers the protein relocalization from the Trans-Golgi Network to the plasma membrane, where the ion excess is exported (Greenough et al. 2004; Petris et al. 2002).

We observe that the experimental findings concerning CTR1 and NRAMP2 do not exclude that, where a Cu restriction should occur, CTR1 and NRAMP2 can play a role in the cell delivery of Cu ions. The affinities of CTR1 (K_m 1-5 μM; Lee et al. 2002) and NRAMP2 (Zerounian and Linder 2002) would discourage such conclusion, unless other surface proteins close to these carriers are able to bind and locally concentrate the ion substrate. The up-regulated prion protein could hold this role by virtue of its high Cu-binding affinity—from femtomolar to nanomolar—within the octameric N-terminal region (Thompsett et al. 2005). So, two steps can be hypothesized for the Cu ion translocation: first, prion proteins concentrate Cu ions within the endocytosis vesicles; second, Cu transport proteins with lower affinity on the walls of vesicles transfer ions into the cytosolic compartments (Salvato B., unpublished manuscript).

If compared to literature, our results demonstrate that the transcriptional responses activated by cell Cu deficiency may depend on the specific cell type. Here, we mainly showed in a neuron-like cell model, overexpressing prion protein, that Cu deprivation triggers the transcriptional up-regulation of PrP^C, playing a role in the modulation of Cu intake and the activation of cell antioxidant defences. We observe that a growing literature (see for a review Mehrpour and Codogno 2010) shows that the overexpression of prion protein is implicated in the malignant progression of many types of cancer. In the light of results presented in this article, the prion protein deposits could be interpreted as a molecular marker of a cell metal imbalance. Further work is evidently needed to clarify this issue, as well as the possible cooperation between prion protein and the other Cu transport systems in driving the cellular ion uptake under both standard and pathological conditions.

Acknowledgement This work was financially supported by MIUR FIRB Project No. RBNE03FMCJ_003 and PRIN 2008 No. 200875 WHMR.

References

Aller SG, Unger VM (2006) Projection structure of the human copper transporter CTR1 at 6-A resolution reveals a compact trimer with a novel channel-like architecture. Proc Natl Acad Sci USA 103:3627–3632

Armendariz AD, Gonzalez M, Loguinov AV, Vulpe CD (2004) Gene expression profiling in chronic copper overload reveals upregulation of Prnp and App. Physiol Genomics 20:45–54

Arredondo M, Muñoz P, Mura C, Nuñez T (2003) DMT1, a physiologically relevant apical Cu^{1+} transporter of intestinal cells. Am J Physiol Cell Physiol 284:C1525–C1530

Arredondo M, Cambiazo V, Tapia L, González-Agüero M, Núñez MT, Uauy R, González M (2004) Copper overload affects copper and iron metabolism in Hep-G2 cells. Am J Physiol Gastrointest Liver Physiol 287:27–32

Bauerly KA, Kelleher SL, Lönnerdal B (2004) Functional and molecular responses of suckling rat pups and human intestinal Caco-2 cells to copper treatment. J Nutr Biochem 15:155–162

Bellingham SA, Coleman LA, Masters CL, Camakaris J, Hill AF (2009) Regulation of prion gene expression by transcription factors SP1 and metal transcription factor-1. J Biol Chem 284(2):1291–1301

Bertinato J, L'Abbé MR (2004) Maintaining copper homeostasis: regulation of copper-trafficking proteins in response to copper deficiency or overload. J Nutr Biochem 15(6):316–322

Blair BG, Larson CA, Adams PL, Abada PB, Safaei R, Howell SB (2010) Regulation of copper transporter 2 expression by copper and cisplatin in human ovarian carcinoma cells. Mol Pharmacol 77(6):912–921

Brown DR (2001) Prion and prejudice: normal protein and the synapse. Trends Neurosci 24:85–90

Brown DR (2003) Prion protein expression modulates neuronal copper content. J Neurochem 87:377–385

Brown DR, Besinger A (1998) Prion protein expression and superoxide dismutase activity. Biochem J 334:423–429

Brown DR, Qin K, Herms JW, Madlung A, Manson J, Strome R, Fraser PE, Kruck T, von Bohlen A, Schulz-Schaeffer W, Giese A, Westaway D, Kretzschmar H (1997a) The cellular prion protein binds copper in vivo. Nature 390:684–687

Brown DR, Schulz-Schaeffer WJ, Schmidt B, Kretzschmar HA (1997b) Prion protein-deficient cells show altered response to oxidative stress due to decreased SOD-1 activity. Exp Neurol 146:104–112

Brown DR, Besinger A, Herms JW, Kretzschmar HA (1998) Microglial expression of the prion protein. NeuroReport 9: 1425–1429

Brown DR, Wong BS, Hafiz F, Clive C, Haswell SJ, Jones IM (1999) Normal prion protein has an activity like that of superoxide dismutase. Biochem J 344:1–5

Brown DR, Nicholas RS, Canevari L (2002) Lack of prion protein expression results in a neuronal phenotype sensitive to stress. J Neurosci Res 67(2):211–224

Cabral AL, Lee KS, Martins VR (2002) Regulation of the cellular prion protein gene expression depends on chromatin conformation. J Biol Chem 277(7):5675–5682

Donnelly PS, Xiao Z, Wedd AG (2007) Copper and Alzheimer's disease. Curr Opin Chem Biol 11:128–133

Francis LW, Lewis PD, Gonzalez D, Ryder TA, Webb G, Joels LA, White JO, Wright CJ, Conlan RS (2009) Progesterone induces nano-scale molecular modifications on endometrial epithelial cell surfaces. Biol Cell 101(8):481–493

Gaeta A, Hider RC (2005) The crucial role of metal ions in neurodegeneration: the basis for a promising therapeutic strategy. Br J Pharmacol 146:1041–1059

Gaggelli E, Kozlowski H, Valensin D, Valensin G (2006) Copper homeostasis and neurodegenerative disorders (Alzheimer's, prion, and Parkinson's diseases and amyotrophic lateral sclerosis). Chem Rev 106:1995–2044

Greenough M, Pase L, Voskoboinik I, Petris MJ, O'Brien AW, Camakaris J (2004) Signals regulating trafficking of Menkes (MNK; ATP7A) copper-translocating P-type ATPase in polarized MDCK cells. Am J Physiol Cell Physiol 287(5):C1463–C1471

Gunshin H, Mackenzie B, Berger UV, Gunshin Y, Romero MF, Boron WF, Nussberger S, Gollan JL, Hediger MA (1997) Cloning and characterization of a proton-coupled mammalian metal ion transporter. Nature 388:482–488

Halliwell B, Gutteridge JM (1984) Oxygen toxicity, oxygen radicals, transition metals and diseases. Biochem J 219:1–4

Halliwell B, Gutteridge JM (1990) Role of free radicals and catalytic metal ions in human disease: an overview. Methods Enzymol 186:1–85

Hardman B, Manuelpillai U, Wallace EM, Monty J-F, Kramer DR, Kuo YM, Mercer JFB, Ackland ML (2006) Expression, localisation and hormone regulation of the human copper transporter hCTR1 in placenta and choriocarcinoma Jeg-3 cells. Placenta 27: 968–977

Harris DA (1999) Cellular biology of prion diseases. Clin Microbiol Rev 12:429–444

Herms J, Tings T, Gall S, Madlung A, Giese A, Siebert H, Schürmann P, Windl O, Brose N, Kretzschmar H (1999) Evidence of presynaptic location and function of the prion protein. J Neurosci 19(20):8866–8875

Jiménez Del Río M, Vélez-Pardo C (2004) Transition metal-induced apoptosis in lymphocytes via hydroxyl radical generation, mitochondria dysfunction, and caspase-3 activation: an in vitro model for neurodegeneration. Arch Med Res 35(3):185–193

Kelleher SL, Lönnerdal B (2006) Mammary gland copper transport is stimulated by prolactin through alterations in Ctr1 and Atp7A localization. Am J Physiol Regul Integr Comp Physiol 291:R1181–R1191

Kessler H, Pajonk F-G, Meisser P, Schneider-Axmann T, Hoffmann K-H, Supprian T, Herrmann W, Obeid R, Multhaup G, Falkai P et al (2006) Cerebrospinal fluid diagnostic markers correlate with lower plasma copper and ceruloplasmin in patients with Alzheimer's disease. J Neural Transm 113:1763–1769

Kim BE, Nevitt T, Thiele DJ (2008) Mechanisms for copper acquisition, distribution and regulation. Nat Chem Biol 4(3):176–185

Kimberlin RH (1974) A comparison of the biochemical changes induced in mouse brain cuprizone toxicity and by scrapie infection. J Comp Pathol 84:263–270

Klamt F, Dal-Pizzol F, Conte da Frota ML, Walz R, Andrades ME, da Silva EG, Brentani RR, Izquierdo I, Fonseca Moreira JC (2001) Imbalance of antioxidant defense in mice lacking cellular prion protein. Free Radical Biol Med 30:1137–1144

Klomp AEM, Tops BBJ, van den Berg IET, Berger R, Klomp LWJ (2002) Biochemical characterization and subcellular localization of human copper transporter 1. Biochem J 364:497–505

Lee J, Prohaska JR, Dagenais SL, Glover TW, Thiele DJ (2000) Isolation of a murine copper transporter gene, tissue specific expression and functional complementation of a yeast copper transport mutant. Gene 254:87–96

Lee J, Peña MMO, Nose Y, Thiele DJ (2002) Biochemical characterization of the human copper transporter Ctr1. J Biol Chem 277(6):4380–4387

Linz R, Lutsenko S (2007) Copper-transporting ATPases ATP7A and ATP7B: cousins, not twins. J Bioenerg Biomembr 39(5–6):403–407

Lombardo MF, Ciriolo MR, Rotilio G, Rossi L (2003) Prolonged copper depletion induces expression of antioxidants and triggers apoptosis in SH-SY5Y neuroblastoma cells. Cell Mol Life Sci 60:1733–1743

Lutsenko S, Petris MJ (2002) Function and regulation of the mammalian copper-transporting ATPases: insights from biochemical and cell biological approaches. J Membr Biol 191:1–12

Mahal SP, Asante EA, Antoniou M, Collinge J (2001) Isolation and functional characterisation of the promoter region of the human prion protein gene. Gene 268(1–2):105–114

Markossian KA, Kurganov BI (2003) Copper chaperones, intracellular copper trafficking proteins. Function, structure, and mechanism of action. Biochemistry 68(8):827–837

Martini LA, Tchack L, Wood RJ (2002) Iron treatment downregulates DMT1 and IREG1 mRNA expression in Caco-2 cells. J Nutr 132(4):693–696

Matsura T, Kai M, Fujii Y, Ito H, Yamada K (1999) Hydrogen peroxide-induced apoptosis in HL-60 cells requires caspase-3 activation. Free Radic Res 30:73–83

Mehrpour M, Codogno P (2010) Prion protein: from physiology to cancer biology. Cancer Lett 290(1):1–23

Monnet C, Marthiens V, Enslen H, Frobert Y, Sobel A, Mège RM (2003) Heterogeneity and regulation of cellular prion protein glycoforms in neuronal cell lines. Eur J Neurosci 18(3):542–548

Moriguchi M, Nakajima T, Kimura H, Watanabe T, Takashima H, Mitsumoto Y, Katagishi T, Okanoue T, Kagawa K (2002) The copper chelator trientine has an antiangiogenic effect against hepatocellular carcinoma, possibly through inhibition of interleukin-8 production. Int J Cancer 102:445–452

Mosmann T (1983) Rapid colorimetric assay for cellular growth and survival: application to proliferation and cytotoxicity assays. J Immunol Methods 65(1–2):55–63

Muller P, van Bakel H, van de Sluis B, Holstege F, Wijmenga C, Klomp LWJ (2007) Gene expression profiling of liver cells after

copper overload in vivo and in vitro reveals new copper-regulated genes. J Biol Inorg Chem 12:495–507
Nazar AM, Silva FA, Amman JJ (1996) Image processing for particle characterization. Mater Charact 36(4):165–173
Nose Y, Rees EM, Thiele DJ (2006) Structure of the Ctr1 copper trans'PORE'ter reveals novel architecture. Trends Biochem Sci 31:604–607
Nose Y, Wood LK, Kim BE, Prohaska JR, Fry RS, Spears JW, Thiele DJ (2010) Ctr1 is an apical copper transporter in mammalian intestinal epithelial cells in vivo that is controlled at the level of protein stability. J Biol Chem 285(42):32385–32392
Ogra Y, Aoyama M, Suzuki KT (2006) Protective role of metallothionein against copper depletion. Arch Biochem Biophys 451: 112–118
Pajonk F-G, Kessler H, Supprian T, Hamzei P, Bach D, Schweickhardt J, Herrmann W, Obeid R, Simons A, Falkai P et al (2005) Cognitive decline correlates with low plasma concentrations of copper in patients with mild to moderate Alzheimer's disease. J Alzheimers Dis 8:23–27
Pattison IH, Jebbett JN (1971a) Clinical and histological observations on cuprizone toxicity and scrapie in mice. Res Vet Sci 12:378–380
Pattison IH, Jebbett JN (1971b) Histopathological similarities between scrapie and cuprizone toxicity in mice. Nature 230:115–117
Pauly P, Harris DA (1998) Copper stimulates endocytosis of the prion protein. J Biol Chem 273:33107–33110
Pena MM, Lee J, Thiele DJ (1999) A delicate balance: homeostatic control of copper uptake and distribution. J Nutr 129:1251–1260
Perera WS, Hooper NM (2001) Ablation of the metal ion-induced endocytosis of the prion protein by disease-associated mutation of the octarepeat region. Curr Biol 11:519–523
Petris MJ, Voskoboinik I, Cater M, Smith K, Kim BE, Llanos RM, Strausak D, Camakaris J, Mercer JF (2002) Copper-regulated trafficking of the Menkes disease copper ATPase is associated with formation of a phosphorylated catalytic intermediate. J Biol Chem 277(48):46736–46742
Petris MJ, Smith K, Lee J, Thiele DJ (2003) Copper-stimulated endocytosis and degradation of the human copper transporter, hCtr1. J Biol Chem 278(11):9639–9646
Pfaffl MW (2001) A new mathematical model for relative quantification in real-time RT-PCR. Nucleic Acids Res 29(9):e45
Rachidi W, Vilette D, Guiraud P, Arlotto M, Riondel J, Laude H, Lehmann S, Favier A (2003) Expression of prion protein increases cellular copper binding and antioxidant enzyme activities but not copper delivery. J Biol Chem 278(11):9064–9072
Ricciardo B, Beddoes K, Sweet M, Nowak A, Crowe A, Nelson D. (2009) Copper chelation retards tumour growth by modulating tumour blood vessels and permitting immune cell infiltration. In: Abstract of the 3rd Western Australia cancer research symposium, Esplanade Hotel, Fremantle, 3 December 2009
Rivera-Mancía S, Pérez-Neri I, Ríos C, Tristán-López L, Rivera-Espinosa L, Montes S (2010) The transition metals copper and iron in neurodegenerative diseases. Chem Biol Interact 186(2):184–199
Rossi L, Marchese E, Lombardo MF, Rotilio G, Ciriolo MR (2001) Increased susceptibility of copper-deficient neuroblastoma cells to oxidative stress-mediated apoptosis. Free Radic Biol Med 30(10):1177–1187
Salès N, Rodolfo K, Hässig R, Faucheux B, Di Giamberardino L, Moya KL (1998) Cellular prion protein localization in rodent and primate brain. Eur J Neurosci 10(7):2464–2471
Santuccione A, Sytnyk V, Leshchyns'ka I, Schachner M (2005) Prion protein recruits its neuronal receptor NCAM to lipid rafts to activate p59fyn and to enhance neurite outgrowth. J Cell Biol 169(2):341–354
Schubert D, Heinemann S, Carlisle W, Tarikas H, Kimes B, Patrick J, Steinbach JH, Culp W, Brandt BL (1974) Clonal cell lines from the rat central nervous system. Nature 249(454):224–227
Song MO, Freedman JH (2005) Expression of copper-responsive genes in HepG2 cells. Mol Cell Biochem 279:141–147
Song I-S, Chen HHW, Aiba I, Hossain A, Liang ZD, Klomp LWJ, Kuo MT (2008) Transcription factor Sp1 plays an important role in the regulation of copper homeostasis in mammalian cells. Mol Pharmacol 74(3):705–713
Song MO, Li J, Freedman JH (2009) Physiological and toxicological transcriptome changes in HepG2 cells exposed to copper. Physiol Genomics 38(3):386–401
Spisni E, Valerii MC, Manerba M, Strillacci A, Polazzi E, Mattia T, Griffoni C, Tomasi V (2009) Effect of copper on extracellular levels of key pro-inflammatory molecules in hypothalamic GN11 and primary neurons. Neurotoxicology 30(4):605–612
Strausak D, Mercer JFB, Dieter HH, Stremmel W, Multhaup G (2001) Copper in disorders with neurological symptoms: Alzheimer's, Menkes, and Wilson diseases. Brain Res Bull 55(2):175–185
Tapiero H, Townsend DM, Tew KD (2003) Trace elements in human physiology and pathology. Copper. Biomed Pharmacother 57(9): 386–398
Tennant J, Stansfield M, Yamaji S, Srai SK, Sharp P (2002) Effects of copper on the expression of metal transporters in human intestinal Caco-2 cells. FEBS Lett 527:239–244
Thompsett AR, Abdelraheim SR, Daniels M, Brown DR (2005) High affinity binding between copper and full-length prion protein identified by two different techniques. J Biol Chem 280(52): 42750–42758
Toni M, Massimino M, Griffoni C, Salvato B, Tomasi V, Spisni E (2005) Extracellular copper ions regulate cellular prion protein (PrPC) expression and metabolism in neuronal cells. FEBS Lett 579(3):741–744
Urso E, Rizzello A, Acierno R, Lionetto MG, Salvato B, Storelli C, Maffia M (2010) Fluorimetric analysis of copper transport mechanisms in the B104 neuroblastoma cell model: a contribution from cellular prion protein to copper supplying. J Membr Biol 233(1–3):13–21
Valentine JS, Gralla EB (1997) Delivering copper inside yeast and human cells. Science 278:817–818
Varela-Nallar L, Toledo EM, Larrondo LF, Cabral AL, Martins VR, Inestrosa NC (2006) Induction of cellular prion protein gene expression by copper in neurons. Am J Physiol Cell Physiol 290:C271–C281
Waggoner DJ, Bartnikas TB, Gitlin JD (1999) The role of copper in neurodegenerative disease. Neurobiol Dis 6(4):221–230
Wright JA, McHugh PC, Stockbridge M, Lane S, Kralovicova S, Brown DR (2009) Activation and repression of prion protein expression by key regions of intron 1. Cell Mol Life Sci 66(23):3809–3820
Yamaji S, Tennant J, Tandy S, Williams M, Srai SKS, Sharp P (2001) Zinc regulates the function and expression of the iron transporters DMT1 and IREG1 in human intestinal Caco-2 cells. FEBS Lett 507:137–141
Yeh K-Y, Yeh M, Watkins JA, Rodriguez-Paris J, Glass J (2000) Dietary iron induces rapid changes in rat intestinal divalent metal transporter expression. Am J Physiol Gastrointest Liver Physiol 279:G1070–G1079
Yu J, Wessling-Resnick M (1998) Influence of copper depletion on iron uptake mediated by SFT, a stimulator of Fe transport. J Biol Chem 273(12):6909–6915
Zatta P, Frank A (2007) Copper deficiency and neurological disorders in man and animals. Brain Res Rev 54:19–33
Zerounian NR, Linder MC (2002) Effects of copper and ceruloplasmin on iron transport in the Caco 2 cell intestinal model. J Nutr Biochem 13:138–148
Zhou B, Gitschier J (1997) hCTR1: a human gene for copper uptake identified by complementation in yeast. Proc Natl Acad Sci USA 94:7481–7486